

1 Globally Significant Mass of Terrestrial Organic Carbon  
2 Efficiently Transported by Canyon-Flushing Turbidity Currents

3 Megan L. Baker<sup>1</sup>, Sophie Hage<sup>2</sup>, Peter J. Talling<sup>1,3</sup>, Sanem Acikalin<sup>4</sup>, Robert G. Hilton<sup>5</sup>,  
4 Negar Haghipour<sup>6,7</sup>, Sean C. Ruffell<sup>3</sup>, Ed L. Pope<sup>1</sup>, Ricardo Silva Jacinto<sup>8</sup>, Michael A.  
5 Clare<sup>9</sup>, Sefa Sahin<sup>4</sup>

6 <sup>1</sup>*Department of Geography, Durham University, Durham, DH1 3LE, UK*

7 <sup>2</sup>*University of Brest, CNRS, IFREMER, Geo-Ocean; 29280 Plouzané, France*

8 <sup>3</sup>*Department of Earth Sciences, Durham University, Durham, DH1 3LE, UK*

9 <sup>4</sup>*School of Civil Engineering and Geosciences, Newcastle University, Newcastle upon Tyne, NE1  
10 7RU, UK*

11 <sup>5</sup>*Department of Earth Sciences, University of Oxford, Oxford, OX1 3AN, UK*

12 <sup>6</sup>*Geological Institute, ETH Zürich, 8092 Zürich, Switzerland*

13 <sup>7</sup>*Laboratory of Ion Beam Physics, ETH Zürich, 8093 Zurich, Switzerland*

14 <sup>8</sup>*Geo-OceanUnit, IFREMER Centre de Brest, 29280 Plouzané, France*

15 <sup>9</sup>*National Oceanography Centre, Southampton, SO14 3ZH, UK*

16 **ABSTRACT**

17 Burial of organic carbon in marine sediments is a long-term sink of atmospheric CO<sub>2</sub> and  
18 submarine turbidity currents are volumetrically the most important sediment transport process on  
19 Earth. Yet the processes, amounts, and efficiency of organic carbon transfer by turbidity currents  
20 through submarine canyons to the deep sea are poorly documented and understood. We present  
21 an organic carbon budget for the submarine Congo Canyon constrained with time-lapse  
22 bathymetry, sediment cores and flow monitoring, including the effects of two >1,000 km runout

23 canyon-flushing turbidity currents. In one year, flows eroded an estimated  $6.09 \pm 2.70$  Mt of  
24 previously-buried terrestrial organic carbon in the canyon, primarily from fine-grained and  
25 vegetation-rich muddy sand facies with high organic carbon contents (up to 11%). The age and  
26 composition of organic carbon in the Congo Canyon is comparable to that in the Congo River,  
27 indicating that transfer is efficient. Over the whole canyon-channel system, we extrapolate that  
28  $43 \pm 15$  Mt of organic carbon was eroded and transported to the deep (> 5 km) sea, equivalent to  
29 22% of the annual global particulate organic carbon export from rivers to oceans, and 54-108%  
30 of the predicted annual terrestrial organic carbon burial in the oceans. Canyon-flushing turbidity  
31 currents carried a globally significant mass of terrestrial organic carbon down just one submarine  
32 canyon in a single year, indicating their importance for redistribution and delivery of organic  
33 carbon to the deep sea.

34

## 35 **INTRODUCTION**

36       Photosynthesis by plants removes  $\text{CO}_2$  from the atmosphere and forms organic matter  
37 containing organic carbon (OC). A fraction of this terrestrial OC travels via rivers to the coast and  
38 is deposited in marine sediments (Blair and Aller, 2012). The burial of OC in marine sediments  
39 over geological timescales leads to a net drawdown of atmospheric  $\text{CO}_2$ , aiding regulation of the  
40 long-term climate (Bernier, 1982; Hilton and West, 2020). It is increasingly recognized that OC  
41 can be efficiently transported and buried in the deep sea by turbidity currents travelling down  
42 active submarine canyons (e.g., Kao et al., 2014; Sparkes et al., 2015; Talling et al., 2024), with  
43 >9,500 canyons worldwide (Harris et al., 2014).

44       Many previous analyses of global OC burial in marine sediments overlooked the role of  
45 turbidity currents and submarine canyons (e.g., Bernier, 1982; Burdige, 2005, 2007). Although

46 many canyons are assumed inactive due to the current sea level high-stand, a number of canyons  
47 in a range of settings have remained active (Covault and Graham, 2010; Heijnen et al., 2022a).  
48 Studies indicate that the mass of OC transported through canyon-channels and buried in submarine  
49 fans (e.g., Bengal Fan, Congo Fan) can be significant (Galy et al., 2007; Rabouille et al., 2019).

50         Sediment and OC within canyons can undergo multiple cycles of erosion, transport and  
51 deposition via relatively small ‘canyon-filling’ turbidity currents, which runout in the canyon-  
52 channel. Occasionally, powerful and long runout ‘canyon-flushing’ turbidity currents erode and  
53 transport material to the depositional lobe (Heijnen et al., 2022b; Pope et al., 2022). Uncertainties  
54 in turbidity current recurrence intervals and runout distance are combined with limited  
55 measurements of quantity, age, and composition of OC in canyon-channel deposits. This has  
56 resulted in a knowledge gap on how turbidity currents move OC within canyons and, crucially, the  
57 potential for OC storage within this part of the global sedimentary system.

58         Here, for the first time, we combine time-lapse seafloor bathymetric maps, sediment cores,  
59 and direct flow-monitoring data to understand how OC is transferred and buried in the deep sea by  
60 turbidity currents. We present a well-constrained OC budget for the Congo Canyon, offshore West  
61 Africa, covering an exceptional one-year period when the canyon experienced two powerful (5-8  
62  $\text{m s}^{-1}$ ) and long (>1,000 km) runout canyon-flushing flows (Talling et al., 2022). Our objectives  
63 are: (1) to show how OC is distributed within the Congo Canyon floor facies and derive an OC  
64 budget for the canyon; (2) upscale the OC canyon budget to quantify the mass of OC eroded from  
65 the Congo Canyon-Channel, and compare this value to global fluxes of terrestrial OC; (3) compare  
66 the Congo Canyon, River and Lobe OC signatures to produce a conceptual model for efficient  
67 transport of terrestrial OC through river-connected submarine canyons.

68

69 **STUDY AREA AND METHODS**

70 The Congo Canyon is directly connected to the Congo River, the second largest river in  
71 the world by discharge, and fifth largest for annual particulate OC export (Fig. 1; Babonneau et  
72 al., 2002; Coynel et al., 2005). In the deeply incised canyon, turbidity currents have been recorded  
73 for ~33% of the time during monitoring periods (Azpiroz-Zabala et al., 2017). At ~2,000 m water  
74 depth the canyon transitions to a less incised channel that continues downslope to the lobe at  
75 ~5,000 m water depth.

76 In September-October 2019, seven piston cores were collected from the canyon thalweg  
77 between 1577 m and 2173 m water depth. The cores were scanned with a Multi-Sensor Core  
78 Logger, split, and visually logged, with five sedimentary facies identified (Fig. 2). Individual beds  
79 could not be correlated between cores due to highly variable deposits. Seventy samples from  
80 different facies were analyzed for grain size. To determine the OC quantity, source (terrestrial or  
81 marine), and age, the same samples were analyzed for total organic carbon (TOC) content, carbon  
82 stable isotope composition ( $\delta^{13}\text{C}$ ) and radiocarbon content (expressed as ‘fraction modern’, Fm, a  
83 measurement of the deviation of the  $^{14}\text{C}/^{12}\text{C}$  ratio of a sample from “modern”; Supplemental  
84 Methods).

85 To record turbidity currents between October 2019 to May 2020, 11 acoustic Doppler  
86 current profiler (ADCP) moorings and 12 Ocean Bottom Seismographs (OBSs) were deployed  
87 along the Congo Canyon-Channel (Fig. 1; Talling et al., 2022; Supplemental Methods). A  
88 powerful turbidity current broke the moorings and two seafloor telecommunications cables on 14-  
89 16<sup>th</sup> January 2020, with the repaired cables broken again by a major flow on 8<sup>th</sup> March 2020.

90 To calculate the Congo Canyon OC budget, the net eroded sediment volume from the  
91 canyon floor was determined using the September-October 2019 and October 2020 multibeam

92 surveys, collected with a Kongsberg EM122 echosounder (Fig. 1). The net eroded sediment  
93 volume was divided into the facies proportions averaged across the sediment cores and converted  
94 to sediment mass, using the average facies porosity  $\pm 1$  standard deviation to get sediment density  
95 (Table S1, S2). The OC mass eroded was calculated using the average TOC  $\pm 1$  standard deviation  
96 for each facies (Table S3). An OC budget for the full Congo Canyon-Channel was estimated using  
97 a facies porosity range and the TOC of Congo Channel sediments from Baudin et al. (2020), and  
98 a total eroded sediment volume of 2.68 km<sup>3</sup> (Talling et al., 2022; Supplemental Methods).

## 99 **RESULTS**

### 100 **Sedimentary facies and organic carbon composition**

101 The Congo Canyon thalweg cores contain five facies, which are now described along with  
102 their OC composition (Figs. 2 and 3; Table S3, S4): (1) **Clay** is homogenous or bioturbated and  
103 comprises 47% of the cores. The facies has a high TOC (reported as the mean,  $\text{TOC}_{\text{av}}$ ,  $\pm 1$  standard  
104 deviation) of  $3.51 \pm 0.60\%$  and an OC age (reported as the mean  $F_m$ ,  $F_{m_{\text{av}}} \pm 1$  standard deviation)  
105 of  $0.94 \pm 0.04$ . (2) **Silt** (18% of the cores) contains occasional laminations or normal grading to  
106 clay and may be homogeneous or bioturbated. This facies has OC  $F_{m_{\text{av}}} = 0.95 \pm 0.02$  and  $\text{TOC}_{\text{av}}$   
107  $= 2.60 \pm 0.99\%$ . (3) **Muddy sand** (22% of the cores) comprises mud with fine- to medium-grained  
108 sand, that may be ungraded or normally graded, and can contain clasts. This has a lower  $\text{TOC}_{\text{av}} =$   
109  $1.81 \pm 1.74\%$ , and older OC ( $F_{m_{\text{av}}} = 0.91 \pm 0.06$ ) compared to clay or silt. (4) **Sand** comprises  
110 clean, fine- to medium-grained sand with rare clasts and is often ungraded or occasionally normally  
111 graded. Sand facies comprises 9% of the cores, with low  $\text{TOC}_{\text{av}} = 0.49 \pm 0.26\%$  and the oldest OC  
112 with  $F_{m_{\text{av}}} = 0.78 \pm 0.06$ . (5) **Vegetation-rich muddy sand** contains concentrated, well-preserved  
113 mm- to cm-sized black wood and plant debris (Fig. 2C) within a fine-grained sand-mud matrix  
114 with no grading. This facies only makes up 4% of the cores but contains high  $\text{TOC}_{\text{av}} = 8.24 \pm$

115 2.24%, and the youngest OC,  $F_{m_{av}} = 0.99 \pm 0.02$ . Most of the facies  $\delta^{13}\text{C}$  values are depleted  
116 ( $-28.5\text{‰}$  to  $-26\text{‰}$ ), indicating a terrestrial origin for the OC, consistent with Congo River  
117 sediment samples (Fig. 3B; Hemingway et al., 2017).

### 118 **Turbidity currents in the canyon**

119 The ADCP-moorings, cable breaks and OBS stations recorded 19 turbidity currents in the  
120 Congo Canyon-Channel over 8 months. The majority (17) of the flows terminated in the canyon  
121 (runout distance  $<190$  km; 2 flows), or before reaching the deep-water channel (runout distance  
122  $<791$  km; 15 flows), with an average  $3.7 \text{ m s}^{-1}$  transit velocity (Fig. S1). However, two turbidity  
123 currents travelled  $>1,000$  km and reached transit velocities of  $5.7$  and  $7.6 \text{ m s}^{-1}$ . These large, cable-  
124 breaking, flows were preconditioned by major river floods (with return intervals of 20-50 years),  
125 but occurred weeks to months after the flood peak, often during spring tides (Talling et al., 2022).

### 126 **Sediment and organic carbon budget**

127 The bathymetric difference map shows significant erosion occurred along the canyon  
128 thalweg over one year (Fig. 1C, D). The net eroded sediment volume along the 112 km-surveyed  
129 length of canyon is  $0.32 \text{ km}^3$ . This equates to  $226 \pm 36$  Mt of sediment and  $6.09 \pm 2.70$  Mt of  
130 terrestrial OC eroded over one year. The clay facies contributed the largest amount of eroded OC  
131 ( $3.13 \pm 0.87$  Mt), followed by silt ( $1.24 \pm 0.60$  Mt), muddy sand ( $0.91 \pm 0.88$  Mt), vegetation-rich  
132 muddy sand ( $0.66 \pm 0.25$  Mt) and sand ( $0.15 \pm 0.09$  Mt; Fig. 3D).

133

## 134 **DISCUSSION**

### 135 **How is organic carbon distributed within the Congo Canyon thalweg?**

136 The Congo Canyon thalweg contains varied sedimentary deposits, with a strong link  
137 between facies type and TOC. The  $\delta^{13}\text{C}$  values indicate that the OC has a terrestrial source. Overall,

138  $6.09 \pm 2.70$  Mt of OC was eroded in the Congo Canyon over one year (Fig. 3). The cores are  
139 dominated by high TOC, fine-grained facies (69% clay and silt) which held 72% of the canyon  
140 OC budget (Fig 3C, D), showing that the canyon of this mud-rich system is primarily fine-grained.  
141 Clay and silt are associated with high TOC values as minerals in these sediments form chemical  
142 bonds with OC, preventing oxidation (Hemingway et al., 2019). The age of the clay and silt OC  
143 ( $F_{m_{av}}$  of  $0.94 \pm 0.04$  and  $0.95 \pm 0.02$ ) likely corresponds to a mixture of young terrestrial biospheric  
144 OC and old terrestrial biospheric OC from degraded organic matter in the Congo Basin, as  
145 indicated by Congo River OC Fm of  $0.89 \pm 0.07$  (Hemingway et al., 2017).

146 The Congo Canyon cores contain only a modest amount of sand (9%) and muddy sand  
147 (18%). These sand-rich facies contained low TOC, and thus provided only 17% of the OC in the  
148 budget (Fig 3D). The sand facies contained the oldest OC in the canyon ( $F_{m_{av}} = 0.78 \pm 0.06$ ). This  
149 suggests large contributions to the bulk Fm measurements from old terrestrial biospheric OC or  
150 petrogenic OC ( $^{14}\text{C}$ -free OC from eroded rocks), as seen in coarse-grained deposits in other  
151 turbidite systems (e.g., Hage et al., 2020).

152 The vegetation-rich muddy sand facies made up only 4% of the total facies yet contributed  
153 11% of the canyon OC budget due to a high  $\text{TOC}_{av}$  of  $8.24 \pm 2.24\%$  (Fig. 3). Prior work in turbidite  
154 systems also concluded that sandy facies can contribute to OC burial in marine sediments due to  
155 plant debris (Lee et al., 2019; Hage et al., 2020). However, these studies observed plant debris in  
156 cleaner-sand turbidite units (i.e.,  $T_B$  and  $T_D$  of the Bouma sequence), rather than the muddy-sand  
157 matrix that contained plant debris in the Congo Canyon. This suggests different hydrodynamic  
158 sorting of plant debris by mud-rich turbidity currents compared to sandy flows. The vegetation-  
159 rich muddy sand had a  $F_{m_{av}} = 0.99 \pm 0.02$ , indicating the dominance of young terrestrial biospheric  
160 OC derived recently from the atmosphere (within the last  $\sim 100$  years). Burial of this fresh material

161 in marine sediments represents a relatively rapid removal of CO<sub>2</sub> from the atmosphere (Lee et al.,  
162 2019).

### 163 **Comparison of organic carbon eroded along the Congo Canyon-Channel to global fluxes**

164 The >1,000 km runout flows eroded 2.68 km<sup>3</sup> of seabed sediment along the Congo Canyon-  
165 Channel (Talling et al., 2022). Facies and TOC trends down the Congo Channel are poorly  
166 constrained. Cores suggest there is a transition from the diverse, TOC-rich canyon sediments to  
167 sandy channel sediments with an estimated TOC of 2.0 ± 0.1%. (Baudin et al., 2010, 2017, 2020).  
168 Using this TOC value for the remaining 2.36 km<sup>3</sup> of eroded sediment, we estimate that 43 ± 15 Mt  
169 of terrestrial OC was eroded along the Congo Canyon-Channel in one year by two canyon-flushing  
170 turbidity currents (Supplemental Methods). This is a globally-significant mass of eroded OC,  
171 equivalent to 22% of annual global particulate OC export from all rivers to the oceans (200  
172 Mt/year; Galy et al., 2015) and 54-108% of the annual terrestrial OC predicted to be buried in the  
173 global ocean (40-80 Mt/yr; Hilton and West, 2020). While the return interval of canyon-flushing  
174 flows and the annual rate of OC transfer by turbidity currents cannot yet be assessed, this study  
175 shows that the mass of terrestrial OC transferred to the deep sea by turbidity currents can contribute  
176 to global OC fluxes.

### 177 **Efficient transport of terrestrial organic carbon through river-connected submarine canyons**

178 Direct monitoring recorded multiple low-velocity ‘canyon-filling’ turbidity currents  
179 terminating in the Congo Canyon-Channel. Two faster, >1,000 km runout, strongly erosive  
180 ‘canyon-flushing’ events were also recorded (Fig. S1). This is consistent with magnitude-  
181 frequency-runout studies of shallow-water turbidity currents (Heerema et al., 2020; Heijnen et al.,  
182 2022b). These flow observations are combined with OC signature data in the Congo River,  
183 Canyon, and Lobe to inform our OC transport model (Fig. 4).



184           The canyon-filling flows rapidly bury sediment and OC in the upper canyon-channel,  
185 helping to protect OC from degradation, and producing high TOC deposits (Fig. 4B; Hedges and  
186 Keil, 1995). Frequent canyon-filling flows may erode and rework the sediment and OC, exposing  
187 the OC to oxygenating conditions. However, despite such reworking, the age and origin of  
188 terrestrial OC in the Congo Canyon ( $F_m = 0.92 \pm 0.08$ ;  $\delta^{13}\text{C} = -26.91 \pm 0.84$ ) is similar to that of  
189 terrestrial OC in the Congo River ( $F_m = 0.89 \pm 0.07$ ;  $\delta^{13}\text{C} = -26.44 \pm 0.77$ ; Hemingway et al.,  
190 2017). This suggests highly efficient OC transport through this part of the system on contemporary  
191 timescales.

192           The OC deposited in the upper canyon-channel is temporarily stored for ~10s of years,  
193 before canyon-flushing flows, triggered by river floods with recurrence intervals of 20-50 years  
194 (Talling et al., 2022), erode the material and quickly transport it to the deep sea, along with  
195 relatively fresh OC from the Congo River floods (Fig. 4C). Flushed material is rapidly deposited  
196 on the lobe, protecting OC from degradation, and sequestering OC for long timescales (Galy et al.,  
197 2007). The Congo Lobe OC age has been measured as  $F_m = 0.89$  and  $F_m = 0.80$  (Savoie et al.,  
198 2009), which is similar to Congo Canyon and River  $F_m$ -values, supporting this model for efficient  
199 OC transport from river-mouth to lobe. Thus, canyon-flushing turbidity currents can efficiently  
200 transport globally significant amounts of terrestrial OC to the deep sea, indicating their importance  
201 for organic carbon budgets.

## 202 **ACKNOWLEDGMENTS**

203           We thank the officers and crew on RRS James Cook. Research was funded by UK NERC  
204 grants NE/R001952/1, NE/V004387/1, NE/R015953/1 and NE/S010068/1, Leverhulme Trust  
205 Early Career Fellowships ECF-2018-267 and ECF-2021-566, and Newcastle University internal  
206 funding. RGH was funded by the Visiting Professor scheme at the Geological Institute, ETH

207 Zürich. SH was funded by the European Union's Horizon 2020 research and innovation  
208 programme under the Marie Skłodowska-Curie grant No 899546.

209

## 210 **REFERENCES CITED**

211 Azpiroz-Zabala, M., Cartigny, M.J.B., Talling, P.J., Parsons, D.R., Sumner, E.J., Clare, M.A.,

212 Simmons, S.M., Cooper, C., and Pope, E.L., 2017, Newly recognized turbidity current

213 structure can explain prolonged flushing of submarine canyons: *Science Advances*, v. 3,

214 doi:10.1126/sciadv.1700200.

215 Babonneau, N., Savoye, B., Cremer, M., and Klein, B., 2002, Morphology and architecture of

216 the present canyon and channel system of the Zaire deep-sea fan: *Marine and Petroleum*

217 *Geology*, v. 19, p. 445–467, doi:10.1016/S0264-8172(02)00009-0.

218 Baudin, F., Disnar, J.R., Martinez, P., and Dennielou, B., 2010, Distribution of the organic

219 matter in the channel-levees systems of the Congo mud-rich deep-sea fan (West Africa).

220 Implication for deep offshore petroleum source rocks and global carbon cycle: *Marine and*

221 *Petroleum Geology*, v. 27, p. 995–1010, doi:10.1016/j.marpetgeo.2010.02.006.

222 Baudin, F., Martinez, P., Dennielou, B., Charlier, K., Marsset, T., Droz, L., and Rabouille, C.,

223 2017, Organic carbon accumulation in modern sediments of the Angola basin influenced by

224 the Congo deep-sea fan: *Deep-Sea Research Part II: Topical Studies in Oceanography*, v.

225 142, p. 64–74, doi:10.1016/j.dsr2.2017.01.009.

226 Baudin, F., Rabouille, C., and Dennielou, B., 2020, Routing of terrestrial organic matter from the

227 Congo River to the ultimate sink in the abyss: a mass balance approach: *Geologica Belgica*,

228 v. 23, p. 41–52, doi:10.20341/gb.2020.004.

229 Berner, R.A., 1982, Burial of organic carbon and pyrite sulfur in the modern ocean: *American*

230 Journal of Science, v. 282, p. 451–473.

231 Blair, N.E., and Aller, R.C., 2012, The Fate of Terrestrial Organic Carbon in the Marine  
232 Environment: Annual Review of Marine Science, v. 4, p. 401–423, doi:10.1146/annurev-  
233 marine-120709-142717.

234 Burdige, D.J., 2005, Burial of terrestrial organic matter in marine sediments: A re-assessment:  
235 Global Biogeochemical Cycles, v. 19, p. 1–7, doi:10.1029/2004GB002368.

236 Burdige, D.J., 2007, Preservation of organic matter in marine sediments: Controls, mechanisms,  
237 and an imbalance in sediment organic carbon budgets? Chemical Reviews, v. 107, p. 467–  
238 485, doi:10.1021/cr050347q.

239 Covault, J.A., and Graham, S.A., 2010, Submarine fans at all sea-level stands: Tectono-  
240 morphologic and climatic controls on terrigenous sediment delivery to the deep sea:  
241 Geology, v. 38, p. 939–942, doi:10.1130/G31081.1.

242 Coynel, A., Seyler, P., Etcheber, H., Meybeck, M., and Orange, D., 2005, Spatial and seasonal  
243 dynamics of total suspended sediment and organic carbon species in the Congo River:  
244 Global Biogeochemical Cycles, v. 19, p. 1–17, doi:10.1029/2004GB002335.

245 Galy, V., France-Lanord, C., Beyssac, O., Faure, P., Kudrass, H., and Palhol, F., 2007, Efficient  
246 organic carbon burial in the Bengal fan sustained by the Himalayan erosional system:  
247 Nature, v. 450, p. 407–410, doi:10.1038/nature06273.

248 Galy, V., Peucker-Ehrenbrink, B., and Eglinton, T., 2015, Global carbon export from the  
249 terrestrial biosphere controlled by erosion: Nature, v. 521, p. 204–207,  
250 doi:10.1038/nature14400.

251 Hage, S. et al., 2020, Efficient preservation of young terrestrial organic carbon in sandy  
252 turbidity-current deposits: Geology, v. 48, p. 882–887, doi:10.1130/G47320.1.

253 Harris, P.T., Macmillan-Lawler, M., Rupp, J., and Baker, E.K., 2014, Geomorphology of the  
254 oceans: *Marine Geology*, v. 352, p. 4–24, doi:10.1016/j.margeo.2014.01.011.

255 Hedges, J.I., and Keil, R.G., 1995, Sedimentary organic matter preservation: an assessment and  
256 speculative synthesis: *Marine Chemistry*, v. 49, p. 81–115, doi:10.1016/0304-  
257 4203(95)00008-F.

258 Heerema, C.J. et al., 2020, What determines the downstream evolution of turbidity currents?  
259 *Earth and Planetary Science Letters*, v. 532, p. 116023, doi:10.1016/j.epsl.2019.116023.

260 Heijnen, M.S. et al., 2022a, Challenging the highstand-dormant paradigm for land-detached  
261 submarine canyons: *Nature Communications*, v. 13, p. 1–11, doi:10.1038/s41467-022-  
262 31114-9.

263 Heijnen, M.S. et al., 2022b, Fill, flush or shuffle: How is sediment carried through submarine  
264 channels to build lobes? *Earth and Planetary Science Letters*, v. 584, p. 117481,  
265 doi:10.1016/j.epsl.2022.117481.

266 Hemingway, J.D., Rothman, D.H., Grant, K.E., Rosengard, S.Z., Eglinton, T.I., Derry, L.A., and  
267 Galy, V. V., 2019, Mineral protection regulates long-term global preservation of natural  
268 organic carbon: *Nature*, v. 570, p. 228–231, doi:10.1038/s41586-019-1280-6.

269 Hemingway, J.D., Schefuß, E., Spencer, R.G.M., Dinga, B.J., Eglinton, T.I., McIntyre, C., and  
270 Galy, V. V., 2017, Hydrologic controls on seasonal and inter-annual variability of Congo  
271 River particulate organic matter source and reservoir age: *Chemical Geology*, v. 466, p.  
272 454–465, doi:10.1016/j.chemgeo.2017.06.034.

273 Hilton, R.G., and West, A.J., 2020, Mountains, erosion and the carbon cycle: *Nature Reviews*  
274 *Earth and Environment*, v. 1, p. 284–299, doi:10.1038/s43017-020-0058-6.

275 Kao, S.J. et al., 2014, Preservation of terrestrial organic carbon in marine sediments offshore

276 Taiwan: Mountain building and atmospheric carbon dioxide sequestration: *Earth Surface*  
277 *Dynamics*, v. 2, p. 127–139, doi:10.5194/esurf-2-127-2014.

278 Lee, H., Galy, V., Feng, X., Ponton, C., Galy, A., France-Lanord, C., and Feakins, S.J., 2019,  
279 Sustained wood burial in the Bengal Fan over the last 19 My: *Proceedings of the National*  
280 *Academy of Sciences of the United States of America*, v. 116, p. 22518–22525,  
281 doi:10.1073/pnas.1913714116.

282 Pope, E.L. et al., 2022, First source-to-sink monitoring shows dense head controls sediment flux  
283 and runout in turbidity currents: *Science Advances*, v. 8, doi:10.1126/sciadv.abj3220.

284 Rabouille, C. et al., 2019, Carbon and silica megasink in deep-sea sediments of the Congo  
285 terminal lobes: *Quaternary Science Reviews*, v. 222, doi:10.1016/j.quascirev.2019.07.036.

286 Savoye, B., Babonneau, N., Dennielou, B., and Bez, M., 2009, Geological overview of the  
287 Angola-Congo margin, the Congo deep-sea fan and its submarine valleys: *Deep-Sea*  
288 *Research Part II: Topical Studies in Oceanography*, v. 56, p. 2169–2182,  
289 doi:10.1016/j.dsr2.2009.04.001.

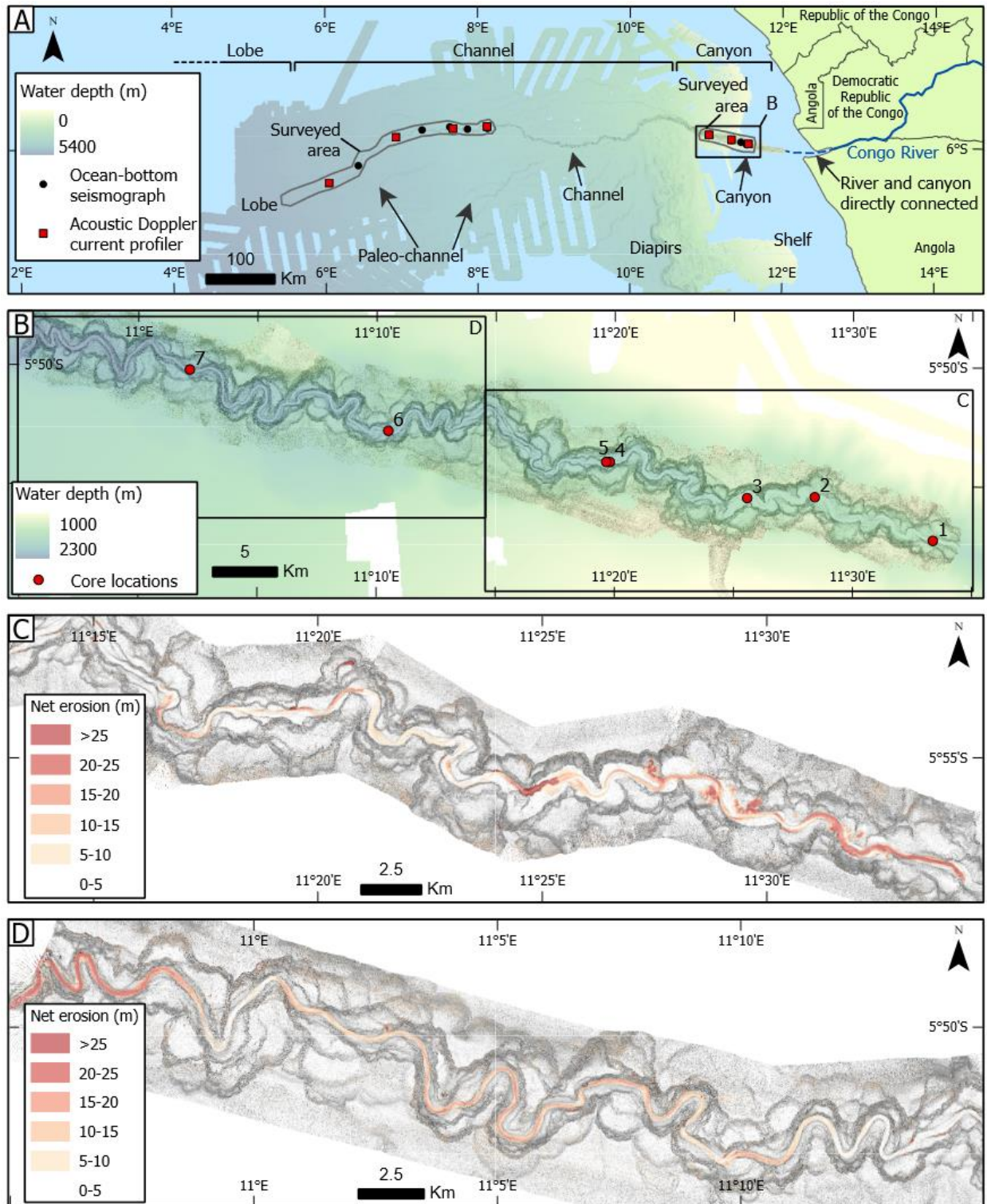
290 Sparkes, R.B., Lin, I.T., Hovius, N., Galy, A., Liu, J.T., Xu, X., and Yang, R., 2015,  
291 Redistribution of multi-phase particulate organic carbon in a marine shelf and canyon  
292 system during an exceptional river flood: Effects of Typhoon Morakot on the Gaoping  
293 River-Canyon system: *Marine Geology*, v. 363, p. 191–201,  
294 doi:10.1016/j.margeo.2015.02.013.

295 Talling, P.J. et al., 2022, Longest sediment flows yet measured show how major rivers connect  
296 efficiently to deep sea: *Nature Communications*, v. 13, p. 1–15, doi:10.1038/s41467-022-  
297 31689-3.

298 Talling, P.J., Hage, S., Baker, M.L., Bianchi, T.S., Hilton, R.G., and Maier, K.L., 2024, The

299 Global Turbidity Current Pump and Its Implications for Organic Carbon Cycling: Annual  
300 Review of Marine Science, v. 16, p. 1–29, doi:10.1146/annurev-marine-032223-103626.

301  
302 FIGURE CAPTIONS

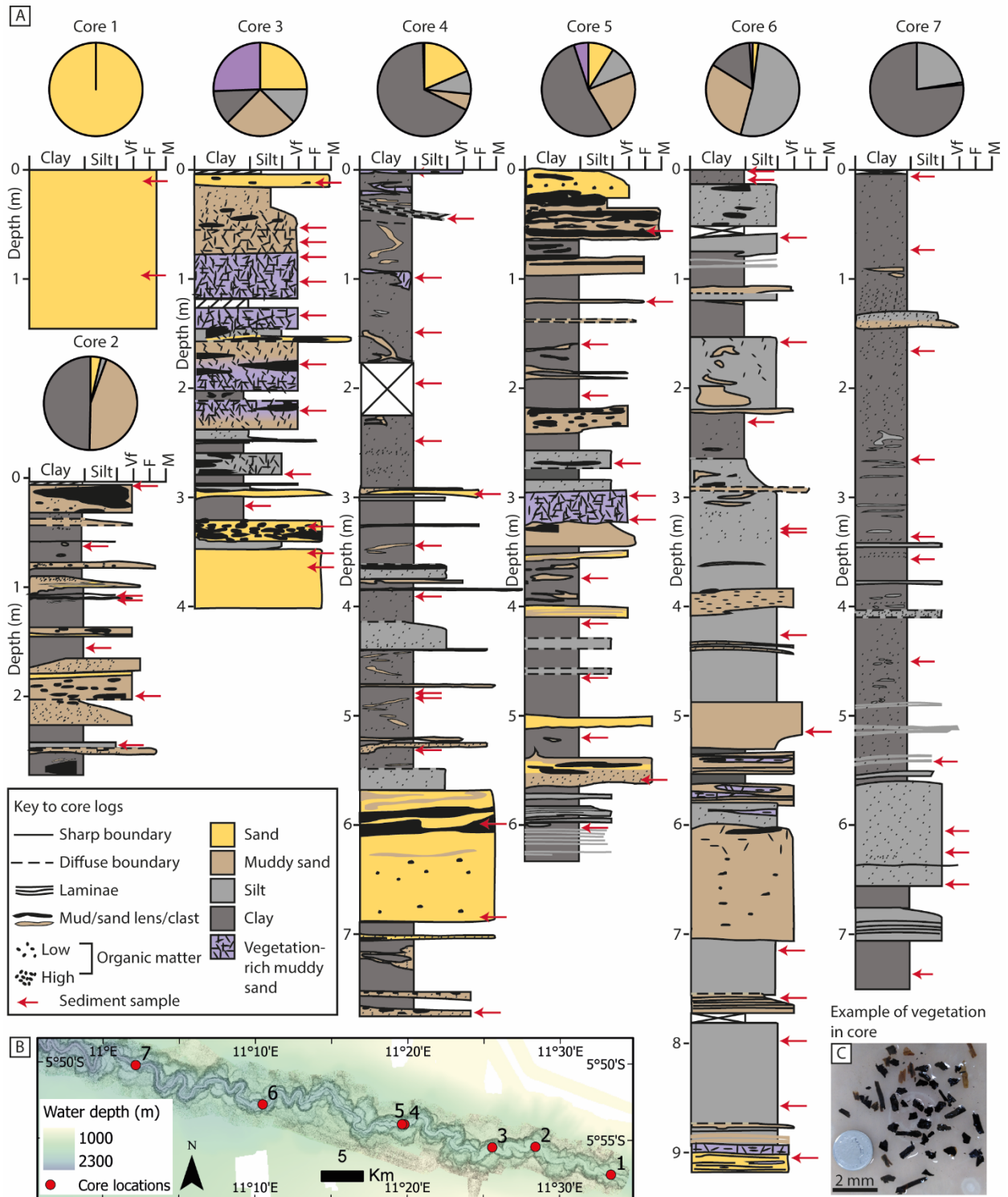


303

304 Figure 1. Study site. A) Bathymetric map of the Congo Submarine Fan (offshore West Africa)

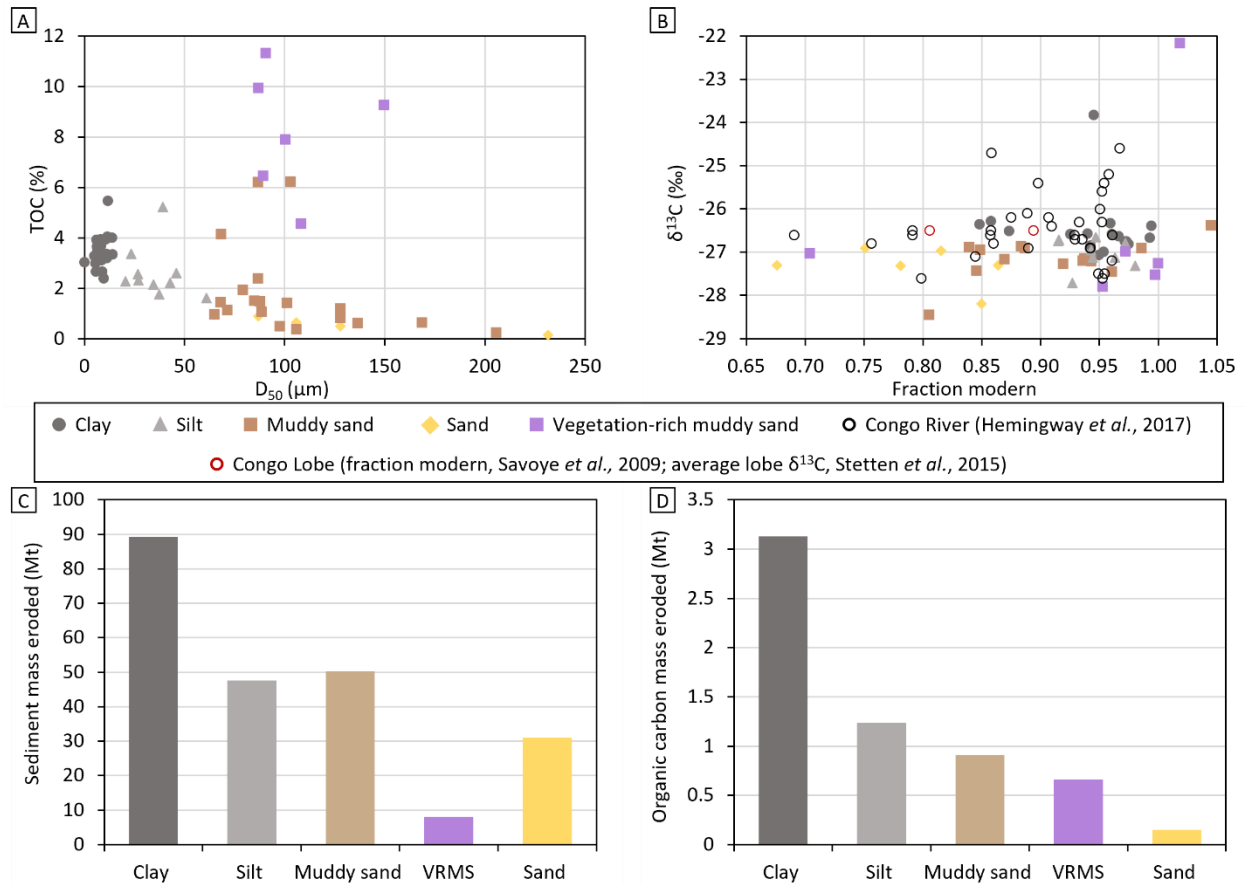
305 and instruments deployed to record turbidity currents. B) 2019 Congo Canyon bathymetry and

306 sediment core sites. C) and D) October 2019 – October 2020 elevation difference map showing  
 307 canyon thalweg net erosion.



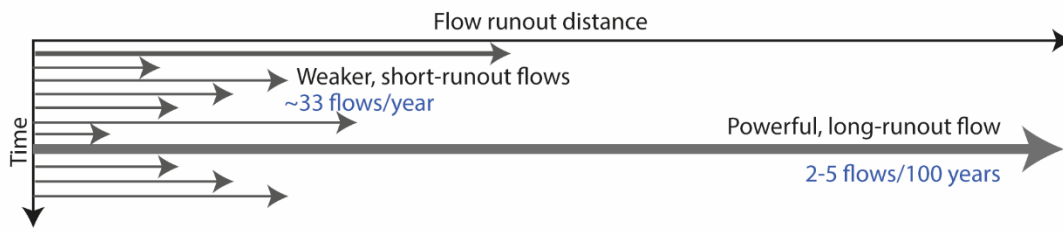


309 Figure 2. Congo Canyon thalweg cores collected October 2019. A) Core logs show the diverse  
 310 range of facies eroded by 2020 canyon-flushing turbidity currents. B) Map of core locations. C)  
 311 Photo of mm-size plant debris in the cores.



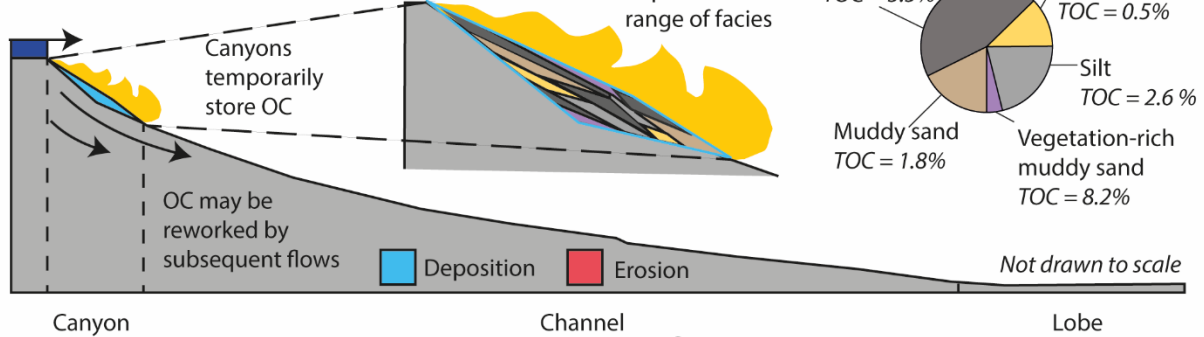
312  
 313 Figure 3. Congo Canyon organic carbon data and budget by facies. A) Total organic carbon  
 314 (TOC) content against median grain size ( $D_{50}$ ). B) Carbon stable isotope ratios ( $\delta^{13}\text{C}$ ) versus  
 315 radiocarbon age (fraction modern), with published data from Congo River and Lobe. C)  
 316 Sediment and D) organic carbon mass eroded from the canyon in one year.

**A) Flow frequency-magnitude-runout in Congo Canyon-Channel**

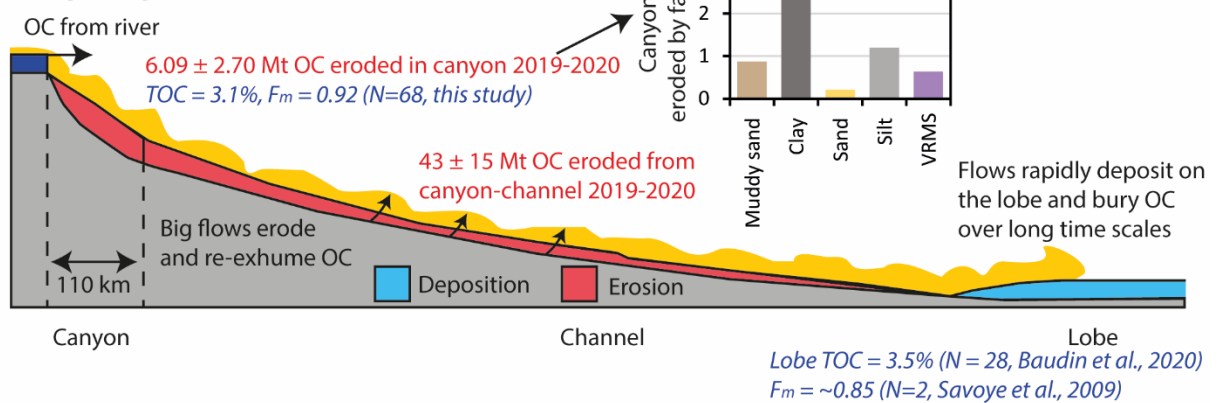


**B) Frequent, small flows**

Congo River exports 2 Mt OC/year  
 TOC = 6.1%,  $F_m = 0.89$  (N= 33, Hemingway et al., 2017)



**C) Infrequent, powerful flows**



317

318 Figure 4. Efficient transport of terrestrial organic carbon (OC) through active submarine canyons

319 connected to rivers. A) Congo Canyon-Channel turbidity currents are mainly ‘canyon-filling’

320 flows with occasional ‘canyon-flushing’ flows. B) Canyon-filling flows deposit sediment and

321 organic carbon in a range of facies. C) Canyon-flushing flows erode and transport sediment and

322 organic carbon to the lobe for long-term burial. VRMS = vegetation-rich muddy sand.

323

324 <sup>1</sup>Supplemental Material. Supplemental Methods (Deployment and specification of monitoring  
325 equipment, turbidity current identification, time-lapse seafloor surveys and analysis of sediment  
326 samples). Tables S1–S5 and Figure S1. Please visit <https://doi.org/10.1130/XXXX> to access the  
327 supplemental material, and contact [editing@geosociety.org](mailto:editing@geosociety.org) with any questions.